DEVELOPMENT OF AN ADVANCED COMPUTATIONAL TOOL FOR START-TO-END MODELING OF NEXT GENERATION LIGHT SOURCES*

J. Qiang† J. Corlett, C. Mitchell, C. Papadopoulos, G. Penn, R. D. Ryne, and M. Venturini,
LBNL, Berkeley, CA 94720, USA

Abstract

Start-to-end simulation plays an important role in designing next generation light sources. In this paper, we present recent progress in a parallel beam dynamics code, IMPACT, towards the fully start-to-end, multi-physics simulation of a next generation X-ray FEL light source. We will discuss numerical methods and physical models used in the simulation. We will also present some preliminary simulation results of a beam transporting through photoinjector, beam delivery system, and FEL radiation.

COMPUTATIONAL FRAMEWORK

The computational framework used for the start-to-end simulation of next generation light sources is the IMPACT code suite. The IMPACT code is a parallel particle-in-cell code suite for modeling high intensity, high brightness beams in rf proton linacs, electron linacs and photoinjectors. It consists of two parallel particle-in-cell tracking codes IMPACT-Z [1, 2] and IMPACT-T [3] (the former uses longitudinal position as the independent variable and allows for efficient particle advance over large distances as in an RF linac, the latter uses time as the independent variable and is needed to accurately model systems with strong space charge as in photoinjectors), an rf linac lattice design code, an envelope matching and analysis code, and a number of pre- and post-processing codes. Both parallel particle tracking codes assume a quasi-electrostatic model of the beam (i.e. electrostatic self-fields in the beam frame, possibly with energy binning for a beam with large energy spread) and compute space-charge effects self-consistently at each time step together with the external acceleration and focusing fields. The 3D Poisson equation is solved in the beam frame at each step of the calculation. The resulting electrostatic fields are Lorentz transformed back to the laboratory frame to obtain the electric and magnetic self-forces acting on the beam. There are six Poisson solvers in the IMPACT suite, corresponding to transverse open or closed boundary conditions with round or rectangular shape, and longitudinal open or periodic boundary conditions. These solvers use either a spectral method for closed transverse boundary conditions, or a convolution-based Green function method for open transverse boundary conditions. The convolution for the most widely used open boundary condition Poisson solver is calculated using an FFT with a doubled computational domain. The computing time of this solver scales like $Nlog(N)$, where N is the number of grid points. The parallel implementation includes both a 2D domain decomposition approach for the 3D computational domain and a particle-field decomposition approach to provide the optimal parallel performance for different applications on modern supercomputers. Besides the fully 3D space-charge capability, the IMPACT suite also includes detailed modeling of beam dynamics in rf cavities (via field maps or z-dependent transfer maps including rf focusing/defocusing), various magnetic focusing elements (solenoid, dipole, quadrupole, etc), allowance of arbitrary overlap of external fields (3D and 2D), structure and CSR wake fields, tracking multiple charge states, tracking multiple bin/bunches, Monte-Carlo simulation of gas ionization, an analytical model for laser-electron interactions inside an undulator, and capabilities for machine error studies and correction.

A SECOND-ORDER PHOTO-ELECTRON EMISSION MODEL

A fast and accurate model is important to simulate the photo-electron emission process for start-to-end light source modeling. In this study, we have developed a second-order computational model to simulate the production of photo-electrons from a photo-cathode driven by an external laser. For a given laser temporal pulse distribution and spatial distribution, a number of electrons equal to the total emitted charge are generated behind the cathode with the same transverse distribution as the laser's and the same longitudinal distribution as the laser's temporal profile times a reference longitudinal velocity v_0. Those electrons are moved outside the photo-cathode during N time steps. Here, the time step size $\Delta t = t_{laser}/N$, where t_{laser} is the total laser pulse length. In the second order photo-electron emission model, the positions and the velocities of an electron after the emission are given by

$$x = x_0 + v_{x0}\delta t_i + \frac{1}{2}a_x(\delta t_i)^2 \quad (1)$$

$$v_x = v_{x0} + a_x\delta t_i \quad (2)$$

$$z = v_{z0}\delta t_i + \frac{1}{2}a_x(\delta t_i)^2 \quad (3)$$

$$v_z = v_{z0} + a_z\delta t_i \quad (4)$$

where $\delta t_i = z_i/v_0$, v_0 is the reference longitudinal velocity, z_i is the electron longitudinal coordinate out of the photocathode right after the emission during the time step Δt, a is the acceleration that can be calculated using the field at the photo-cathode surface. The y position and velocity can be obtained by replacing the x with the y in above equations. In the following, we generate 300 pC photo electrons

* Work supported by the U.S. Department of Energy under Contract No. DE-AC02-05CH11231.

† jqiang@lbl.gov

ISBN 978-3-95450-115-1

from a photo-injector gun using the second-order emission model and the first-order emission model without including acceleration. The current profile of the beam shortly after the emission is shown in Figure 1 using different emission steps of the above emission models. It is seen that the crude

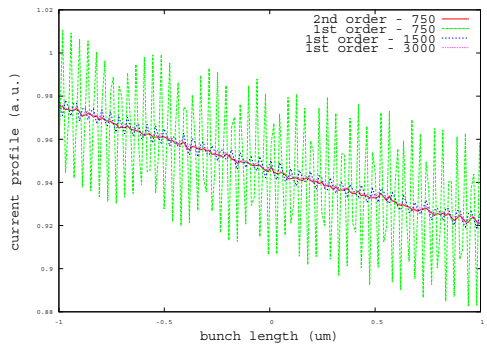

Figure 1: A section of current profile of the beam after the emission using the second-order emission model and the first-order emission model with different emission steps.

first order emission model can introduce aritifial modulation of the beam. A much larger number of emission steps (a factor of 4) i.e. smaller emission step size, are needed in order to achieve the same level smoothness of the current profile.

IMPROVED COHERENT SYNCHROTRON RADIATION MODEL

Accurate simulation of the beam energy loss, induced energy spread, and microbunching effects of coherent synchrotron radiation (CSR) is of central importance to the modeling of future light sources. We have developed and implemented an Integrated Green Function (IGF) method for computing CSR wakefields based on the 1D model of [4]. This model accurately includes short-range wakefield effects, is accurate over a large range of energies, and includes transient wakefields due to the bunch entering and exiting a bend. An additional IGF routine based on the model of [5] has also been developed that can treat the effect of radiation that has propagated from upstream across multiple beam-line elements.

In the integrated Green function method, the 1D charge density λ is approximated by a piecewise polynomial of fixed degree, and the CSR wake integral is performed analytically [6]. As a result, the accuracy of this technique does not depend on how well one resolves the rapidly-varying integral kernel, but instead depends only on how well one resolves the longitudinal charge density. In addition, this method does not involve computing the derivative $d\lambda/dz$, which may require artificial smoothing due to the presence of numerical noise. Fig. 2 shows a comparison between results obtained using the IGF method and results obtained using several common 1D CSR models [4, 7, 5], demonstrating good agreement. Shown are results obtained using direct integration of the CSR wake integral of [4] with 104312 points (red), using the IGF method based on [4] using 1024 points (green), using the IGF method based on [5] using 1024 points, and using the method of [7] with 1024 points (purple). The curves are indistinguishable except the curve based on [7].

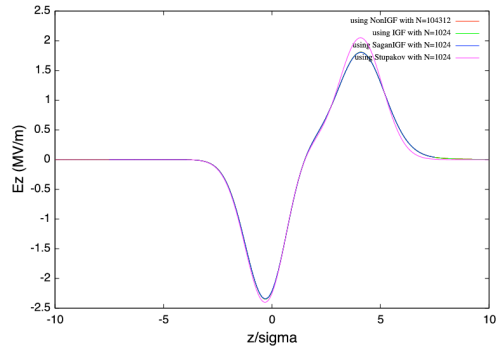

Figure 2: Comparison between the CSR wake computed using several 1D methods for the parameters in Fig. 3 of [7].

The importance of including CSR from upstream bends is demonstrated in Fig. 3. We computed CSR wakefields throughout a chicane that has been proposed for magnetic bunch compression as part of a next generation X-ray FEL. The two central bends have a common bending angle of 89 mrad and are separated by a drift of 5 m. As a bunch travels through the downstream bend, particles in the bunch will encounter radiation generated within this bend ("downstream CSR"), as well as radiation that was generated upstream within the previous bend ("upstream CSR"). Fig. 3 illustrates the wakefield due to upstream CSR along the length of a Gaussian bunch, at various angles into the second bend. The bunch energy is taken to be 250 MeV, the bunch charge is 0.3 nC, and the rms bunch length is $\sigma = 577\mu$m. The normalization is given by $W_0 = 28.2$ keV/m. Despite the large drift separation of 5 m, the peak value of the CSR due to the upstream bend is 39%, 132%, and 126% of the peak value of the total CSR, respectively.

START-TO-END SIMULATION USING REAL NUMBER OF ELECTRONS

The time-dependent IMPACT-T code, the position-dependent IMPACT-Z code, and the FEL X-ray radiation GENESIS code are integrated into a single code to facilitate full start-to-end simulations with a real number of electrons (about 2 billions in this study). Here, the IMPACT-T code is used to simulate the photo-electron production and accleration inside the photo-injector. The IMPACT-Z code is used to simulate the electron beam acceleration, compression and transport through the linac and spreader. The GENESIS code [10] is used to self-consistently simulate FEL X-ray radiation inside an undulator. The self-consistent 3D space-charge effects, the accelerating cavity structure wakefields, and the CSR wakefields are included in the IMPACT code simulation. The macroparti-

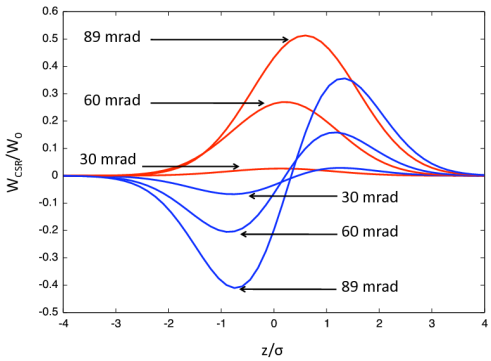

Figure 3: (Blue) The total CSR wake within the third bend of the NGLS chicane [8], shown when the bunch centroid is located 30, 60, and 89 mrad into the bend. The peak value of the wake increases as the bunch moves farther into the bend. (Red) Contribution to the CSR wake due to radiation emitted from the previous bend, located 5 m upstream.

cle electrons pass from the one code to the other code directly through the internal memory of the supercomputer. As an illustration of this start-to-end capability, i.e. from the photo-cathode to the end of undulator, we simulated a next generation X-ray light source with 300 pC electrons that is being studied at LBNL [9]. Figure 4 shows the beam current profile and sliced emittances at the end of the accelerator beam delivery system. It is seen that the peak current reaches about 900 A. The sliced emittances are about 0.7 mm-mrad. Figure 5 shows the averaged 1 nm X-ray radation power along the undulator distance and X-ray radiation temporal profile at the end of the undulator.

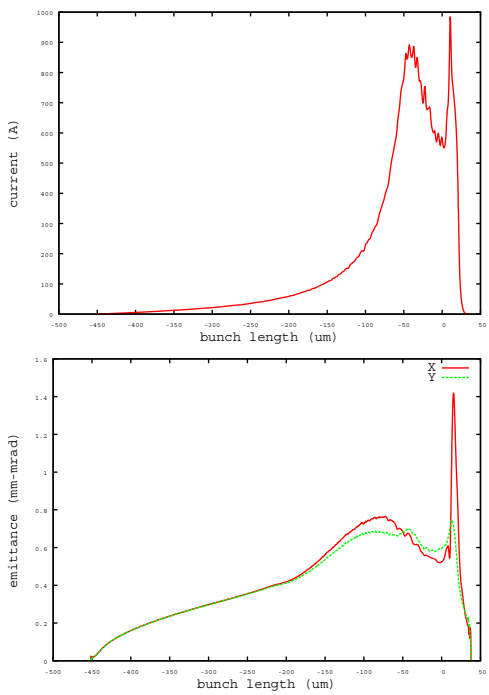

Figure 4: The electron beam profile (top) and sliced emittances at the end of the accelerator beam delivery system.

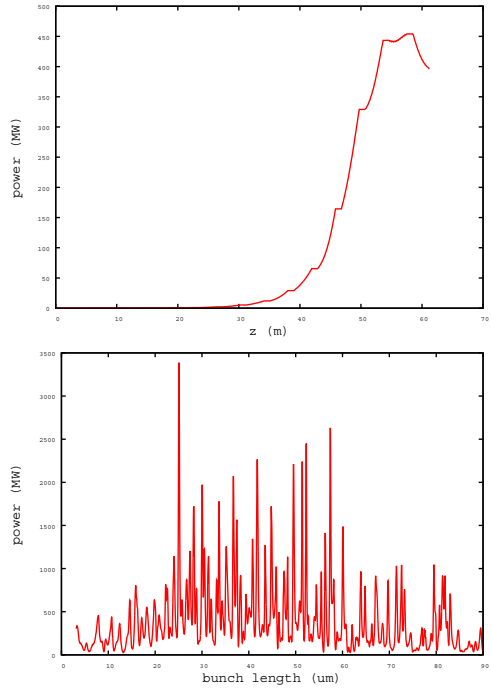

Figure 5: The averaged 1 nm X-ray radation power along the undulator distance (top) and X-ray radiation temporal profile at the end of the undulator (bottom).

ACKNOWLEDGEMENTS

This research used computer resources at the National Energy Research Scientific Computing Center.

REFERENCES

[1] J. Qiang et al., J. Comp. Phys. vol. 163, 434, (2000).

[2] J. Qiang et al., Phys. Rev. ST Accel. Beams 12, 100702 (2009).

[3] J. Qiang et al., Phys. Rev. ST Accel. Beams, 9, 044204 (2006).

[4] E. L. Saldin et al., Instrum. Meth. Phys. Res. A **417**, 158 (1998).

[5] D. Sagan et al., Phys. Rev. ST-Accel. Beams, **12**, 040703 (2009).

[6] R. D. Ryne, B. Carlsten, J. Qiang, and N. Yampolsky, http://arxiv.org/abs/1202.24009.

[7] G. Stupakov and P. Emma, Proceedings of EPAC 2002, Paris, France, 1479 (2002).

[8] M. Venturini et al, "Beam Dynamics Studies of a High-repetition Rate Linac Driver for a 4th-generation Light Source," this conference.

[9] J. Corlett, et al., "Next generation light source R&D and design studies at LBNL," this conference.

[10] S. Reiche, Nucl. Instrum. Methods Phys. Res. A 429, 243 (1999).

ISBN 978-3-95450-115-1